

Conference Title

## Research on the Output Characteristics of IPMSM according to the Pole-Slot Combinations

Choe You-Young<sup>1</sup>, Lee Ki-Doek<sup>1</sup>, Jang Ik-Sang<sup>1</sup>, Kim Mi-Jung<sup>1</sup>, Ham Sang-Hwan<sup>2</sup>, Lee Ju<sup>1a</sup>, Ko Kwang-Cheol<sup>1a</sup> <sup>a\*</sup>

<sup>1</sup>*Hanyang University, 17 Haengdang 1-dong, Seongdong-gu, Seoul, 133-791, South Korea*

<sup>2</sup>*Sunchon First College, 17 Jeildaehak-gil Suncheon, Jeonnam, 540-744, South Korea*

---

### Abstract

Due to the global energy depletion and environmental problems, engine cars are currently being replaced by hybrid and electric cars. Military engine trucks must also be replaced by hybrid trucks because the former need improved starting performance, a high power supply, and low-noise operation, apart from environmental reasons.

Compared to SPMSM (surface-mounted permanent-magnet synchronous motor), IPMSM (interior permanent-magnet synchronous motor) can use a reluctance-torque-caused salient pole as well as a magnetic torque; as such, IPMSM has a high power density. It can also be made lightweight and can be made to have high-speed operation through field-weakening control. For these reasons, IPMSM is currently being used as the traction motor of hybrid and electric vehicles. In this paper, an IPMSM for Hybrid Humvee is introduced. The characteristics of four models with constraint conditions are analyzed according to the pole-slot combinations. After the analysis of the designed motors, the resulting values are compared with one another.

© 2011 Published by Elsevier Ltd. Selection and/or peer-review under responsibility of the organizing committee of 2nd International Conference on Advances in Energy Engineering (ICAEE). Open access under [CC BY-NC-ND license](https://creativecommons.org/licenses/by-nc-nd/4.0/).

Keywords: IPMSM, traction motor, hybrid vehicle, electric vehicle, slot, pole

---

### 1. Introduction

The traction motor has to satisfy the required output characteristics with the voltage and current limits by using a battery and an external diameter limit. Moreover, a low torque ripple and a cogging torque are required. As the torque ripple and the cogging torque cause noise, vibration, mechanical stress, etc., the

---

\* Corresponding author. Tel: +82-2-2220-0342. Fax: +82-2-2220-7775

E-mail address: [julee@hanyang.ac.kr](mailto:julee@hanyang.ac.kr), [kwang@hanyang.ac.kr](mailto:kwang@hanyang.ac.kr)

determination of the pole-slot combinations in the basic design is very important in designing a traction motor that satisfies the high power density, low torque ripple, and cogging torque requirements. To determine the output characteristics of the interior permanent-magnet synchronous motor (IPMSM) according to the pole-slot combinations, an about-100kw IPMSM was introduced in this study.

## 2. Design of the Basic Model

### 2.1 Load conditions

The load that occurs when a vehicle is running consists of the rolling resistance by friction, the air drag resistance by a fluid, and the slope resistance by a gradient. First, all the resistances have to be calculated. Consequently, the load conditions need a high torque and a wide speed range. To satisfy the load conditions shown in Fig. 1, the traction motor needs output characteristics that satisfy points 1 and 2. The region between 0 rpm and point 1 is called the *constant torque region*, and the region between points 1 and 2 is called the *constant power region*.

This paper introduces the 119kw-class IPMSM, which satisfies the 400 Nm torque at 2843 rpm and the 50 Nm torque at 10000 rpm.

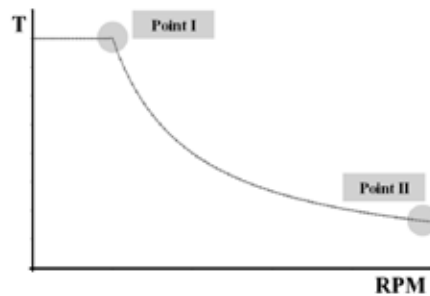


Figure 1. Output conditions of IPMSM for Hybrid Humvee.

### 2.2 Design conditions and constraints of the model

To compare the output characteristics according to the slot-pole combinations, equation (1) was examined. It consists of product output coefficients  $C_{om}$  and  $D_g^2 L_{stk}$ .

$$T = C_{om} D_g^2 L_{stk} \quad \because C_{om} = \frac{\pi}{4} k_w \hat{B}_g a c, \quad (1)$$

where the torque equation and output coefficient  $C_{om}$  represent a case of salient pole ratio 1.

As the motor size is proportional to the rotor size (volume), it is also proportional to the torque and to the specific loadings. First, the product of a winding factor and a specific magnetic as well as electric loading are dealt with as constants, which allows the rotor size to be determined automatically. Eventually, to compare the output characteristics according to the slot-pole combinations, stator shape design was performed.

The number of poles was restricted by the max rpm of point 2 and a switching frequency represented in Table 1. In the 10 kHz switching frequency, a high-speed operation (e.g., 10000 rpm) reduces the controllability. For this reason, this paper deals with four and eight poles (4p and 8p).

In other words, the design conditions are the same in terms of the magnet volume, rotor size, and 4p and 8p. Further, to compare the concentrated winding with the distributed winding, 4p/6 slots (6s), 4p/18s, 8p/12s, and 8p/36s were considered.

**Table 1. Design Specifications of the Four Models**

Parameters	Value
Power	119 kw
Torque @ base rpm	400 Nm @ 2843 rpm
Torque @ max rpm	50 Nm @ 10000 rpm
DC link voltage	Phase voltage peak: 392 V
Current density	15A peak/mm <sup>2</sup> (water cooling)
IGBT	Under 900 A/10 KHz
Temperature	170°C
Core	35PN230 (S08)
Rotor/stack/airgap	260/230/1 mm
Permanent magnet	Br: 1.25 T@20°C; $\mu_r$ : 1.05, Temperature coefficient of Br: -0.095%/°C
Magnet volume	304*10*250 mm

### 2.3 Design of the four models

The four basic models that had been designed based on the magnetic equivalent circuit was verified via FEM (finite-element method). To determine the output characteristics and the 1.6T magnetic saturation at the yoke and teeth of the stator, the optimum design was created after the basic design. The optimum designs of the four basic models are shown in Fig. 2.

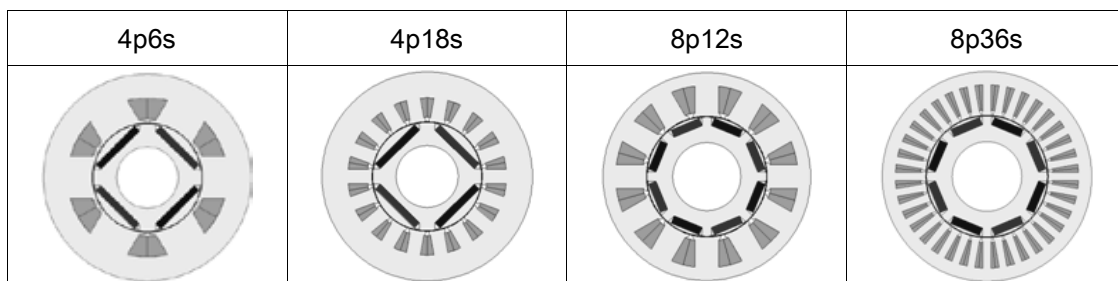


**Figure 2. Optimum designs of the four basic models.**

### 2.4 Comparison of the output characteristics of the design models

To make the output characteristics of all the models equal, the rotor volume and the magnet volume were fixed. To satisfy the output characteristics with the current density of 15 A peak/mm<sup>2</sup>, the current

and the slot area were changed according to the magnetic saturation in the stator yoke and teeth. Consequently, the optimum models have the same output characteristics but different sizes. Their power densities and torques per volume were compared, respectively.

$$W_{sy} = \frac{\phi_g}{2B_{ym}L_{stk}}, \quad (2)$$

where  $W_{sy}$  : width of the stator yoke;

$B_{ym}$  : saturation flux density at the stator yoke;

$L_{stk}$  : stack length; and

$\phi_g$  : flux per pole.

As  $\phi_g$  was changed according to the pole number, the width of the stator yoke was also changed. Consequently, the motor volumes of the 4p and 8p models are different.

**Table 2. Output Characteristics of the Four Models**

Parameters	4p6s	4p18s	8p12s	8p36s
Torque (Nm) @ base rpm	404.29	401.66	405.82	402.27
Torque (Nm) @ max rpm	123.52	121.58	240.45	229.34
Stator diameter (mm)	147.5	144.6	130.3	128.9
Torque (Nm)/volume (cm <sup>3</sup> )	0.0795	0.0805	0.0903	0.0905

## 2.5 Comparison of the cogging torques and torque ripples of the four models

The torque pulsation includes the cogging torque and the torque ripple. The cogging torque occurs when a current is not applied, and the torque ripple is caused by the inductance fluctuation according to the rotor position and the interaction between the magnetomotive force of the stator and the permanent magnet. If the cogging torque and torque ripple sufficiently increase, the accuracy of the motor control decreases, and noise and vibration are caused. Fig. 3 and Table 3 show the cogging torques and torque ripples of the four models.

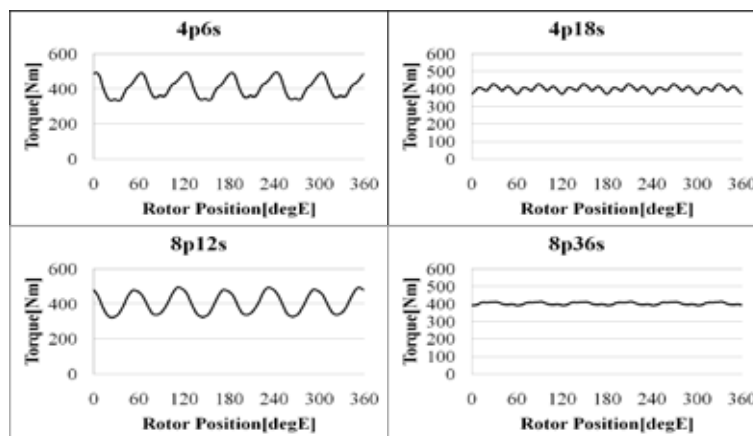


**Figure 3. Torque ripples of the four models.****Table 3. Cogging Torques and Torque Ripples of the Four Models**

	<b>4p6s</b>	<b>4p18s</b>	<b>8p12</b>	<b>8p36s</b>
Cogging torque pk-pk (Nm)	8.300	9.075	1.547	1.212
Torque ripple pk-pk (Nm)	157.9	58.47	172.7	22.1

The cogging torque and torque ripple of the distributed winding are smaller than those of the concentrated winding, but the concentrated winding has many advantages. As the slot fill factor of the concentrated winding is generally bigger than that of the distributed winding, the power density of the concentrated winding is superior to that of the distributed winding. Moreover, the end turns of the concentrated winding are lower than those of the distributed winding. Thus, the copper loss and stack length of the concentrated winding are lower than those of the distributed winding. Both winding methods have advantages by case.

## 2.6 Comparison of the losses of the four models

In this study, the copper loss, which accounts for the biggest part of the motor loss; the core loss, which is produced by the stator and rotor; and the eddy current loss, which is produced by the permanent magnet, were compared. The copper loss was calculated using a resistance of the stator winding and current. The loss produced by the stator and rotor at 2843 rpm, the base rpm in FEM, was compared with the loss data of each frequency. Lastly, a large permanent-magnet machine has a fairly large eddy current loss due to the existence of conductivity on the permanent magnet. In this study, the permanent magnet was examined via lamination. Comparing the distributed winding and concentrated winding, the end turn was longer in the distributed winding. Thus, the phase resistance of the distributed winding was bigger than that of the concentrated winding, but the concentrated winding needed a higher current for the same torque. Thus, the copper loss of the concentrated winding was bigger than that of the distributed winding.

**Table 4. Losses of the Four Models**

<b>Loss</b>	<b>4p6s</b>	<b>4p18s</b>	<b>8p12s</b>	<b>8p36s</b>
Phase resistance ( $\Omega$ )	0.0136	0.0143	0.001	0.0104
Copper loss (W)	4715.9	3774.8	3589.6	3156.8
Core loss (W)	824.77	750.63	1056	1019.9
Eddy current loss (W)	97.278	1.0127	51.764	0.921

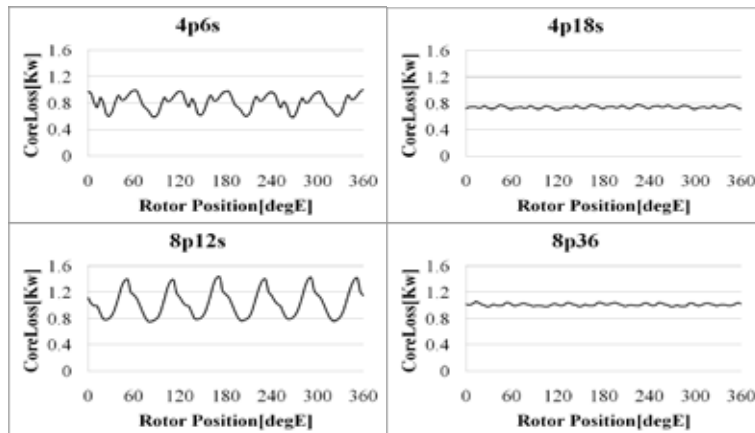


Figure 4. Core losses of the four models.

### 3. Conclusion

In this study, the pole-slot combinations that were restricted by the interior permanent-magnet synchronous motor for Hybrid Humvee were selected. Optimum design was performed via FEM after the designing of the four basic selected-combinations models based on the magnetic equivalent circuit. It was possible to compare the cogging torques and the torque ripples by examining the differences in the sizes and slots of the distributed winding and concentrated winding by varying the numbers of poles and slots. Lastly, the copper loss was calculated by considering the operating temperature, and the core loss and eddy current loss were compared by considering the core loss data of the material and the conductivity of the permanent magnet.

### Acknowledgment

This work was supported by Human Resources Development of the Korea institute of Energy Technology Evaluation and Planning(KETEP) grant funded by the Korea government Ministry of Knowledge Economy(No. 2009EAPHMP010000)

### References

- [1] Tomas M. Jahns, "DESIGN, ANALYSIS, AND CONTROL OF INTERIOR PM SYNCHRONOUS MACHINES", October 2004.
- [2] Katsumi Yamazaki, "Effect of Eddy Current Loss Reduction by Segmentation of Magnets in Synchronous Motors: Difference Between Interior and Surface Types", IEEE TRANSACTIONS ON MAGNETICS, VOL. 45, NO. 10, OCTOBER 2009